

WHERE ARE THE LONE-PAIR ELECTRONS IN SUBVALENT FOURTH-GROUP COMPOUNDS?

S.-W. NG¹ and J. J. ZUCKERMAN

Department of Chemistry, University of Oklahoma, Norman, Oklahoma

I. Introduction	297
II. Divalent Fourth-Group Structures	299
III. History	302
IV. Symmetrical Subvalent Systems	304
A. Molecular	304
B. Extended Lattices	307
V. Conclusions	319
References	321

I. Introduction

In July 1983 we began to collect the literature describing the structures of subvalent compounds of the main fourth-group elements, hereafter designated generically as E. Our goal at that time was to provide in one place a complete and up-to-date source of structural information from methods capable of yielding internuclear distances and angles for these systems, from carbon to lead. This file has now grown to over 1500 references ranging from material on carbenes and transition metal carbene complexes to crystallographic studies on the heavier fourth group congeners found in the mineralogical literature.

A subsidiary goal from the outset was to identify those systems in which the lone-pair electrons present in these subvalent species show no stereochemical activity; that is, in which the fourth-group atoms occupy sites of perfect symmetry in the solid state. Our search brought forth various scattered examples of such structural systems, and reading of their unusual properties heightened our interest. However, with the fortuitous synthesis by C. Janiak in our own laboratory

¹ Present address: Institute of Advanced Studies, University of Malaya, Pantai Valley, Kuala Lumpur, Malaysia.

of a molecular example in decaphenylstannocene (77), $[\eta^5\text{-(C}_6\text{H}_5)_5\text{C}_5\text{]}_2\text{Sn(II)}$ (see Section IV,A,3), we decided that it would be useful to draw attention to these systems by preparing a shorter review devoted entirely to this subject.

The enumeration and description of the symmetrical subvalent species before you are restricted to those in which the lone-pair electrons are totally inert stereochemically; that is, in which the geometry at the fourth-group atom reflects the situation expected for one fewer electron pair than is in fact present. The evidence we regard as acceptable for authenticating this situation is limited to that deriving from methods yielding precise internuclear distances and angles, primarily single-crystal X-ray diffraction with some neutron, gas-phase, and solid state electron diffraction. The structural formula serves to specify the subvalent nature of the fourth-group species.

Caution must be exercised in using much of the earlier gas-phase electron diffraction data in view of limitations on instrumentation and experimental and computational methods which often required that implicit assumptions about portions of the molecular geometry be made. Unfortunately as well, many of the early X-ray studies lack the accuracy required to draw definite conclusions about the geometry of the E(II) coordination sphere because of the inability to locate precisely lighter atoms in the presence of the heavy E atom. The caveat of Jones (89) regarding even modern results has been extremely useful in guiding our efforts to interpret the literature. The difficulties in interpreting vibrational spectra in terms of structure are well known and rule out their use for our purposes. Likewise, the absence of resolvable quadrupole splitting (QS) in tin-119m Mössbauer spectra may not be used to specify perfect cubic symmetry since small splittings may not be detected in the relatively broad resonance lines. Some quite low symmetry structures give sharp spectral singlets (177, 178). The same is true of single nuclear quadrupole resonance (NQR) signals suggesting high symmetry sites; the other (weaker) lines may just not have been detected. The converse is not true, however. Spectroscopic evidence of lowered symmetry, if reliable, must be regarded seriously since these techniques may operate on a more rapid timescale and not be subject to the averaging involved in recording crystallographic data (see below).

If in a complex the direct neighbor nuclei have the same atomic number and are located at identical distances from the central atom, then the coordination number of this atom can be specified exactly. Complexes with identical ligands are called homoleptic. However, when the nearest neighbor nuclei are not identical, the distances from the central atom will be different, although those nuclei may still be located on the Cartesian coordinates. In these heteroleptic complexes, specify-

ing the complete absence of stereochemical activity on the part of a lone pair of electrons on the central atom becomes less certain, even when the distances to the nearest neighbor nuclei are similar. When the various distances differ by larger amounts, the value of the coordination number of the central atom is itself thrown into doubt as well. Generally, internuclear distances at most 10% longer than the shortest tend to be taken into account in determining the coordination number. Since our goal is to enumerate the cases in which a lone pair of electrons on a central atom is totally inert stereochemically, we will confine our attention to the homoleptic complexes only, and further to those cases in which the E(II) atom is located at the exact center of a perfect polyhedron. For two and three coordination we seek linear and trigonal-planar arrangements, for four coordination the tetrahedron or the unknown square plane, for five coordination the familiar trigonal bipyramid, and for six coordination the octahedron. While for 8 and 12 coordination the cube or square antiprism and cube octahedron or dodecahedron, respectively, are available, for 7, 9, 10, and 11, coordination it is more difficult to specify the regular shapes sought. Moreover, since the energy differences between the coordination numbers 7-12 are generally small, solid-state data reveal many examples of situations in which the coordination number appears to be intermediate. This is especially true the larger the central atom. Transformations among the choices of idealized geometries are often comparable with the distortions imposed by vibrationally excited states. Thus, for experimental results from techniques involving long-term observation or averaging ($>10^{-2}$ sec), the structures should be considered as stereochemically nonrigid species. Thus solid-state optical activity having its origin the central atom may be short-lived in solution, and geometrical isomerization may be also a low-energy barrier process, with smaller differences than packing forces in the solid state, solvation energies in the solution state, or association energies in the liquid state (122).

It should be recalled that the solution of crystal structures by diffraction techniques involves at least two kinds of averaging, the time average and the average content of the unit cell. Other techniques which observe on a shorter time scale may legitimately suggest a lower local symmetry in the same phase than that obtained by crystallography.

II. Divalent Fourth-Group Structures

The divalent state does not usually enter into carbon or silicon chemistry except at high temperatures or where transient reaction

intermediates are involved. However, a number of Ge(II) derivatives are stable at ambient temperature, and the prevalence of the subvalent state increases with Sn(II) (38, 67) and Pb(II).

The elements in their lower oxidation states are less electronegative, and comparable bonds are longer. While all the heavier main-group elements form compounds in an oxidation state two units lower than their group number, no compelling and comprehensive explanation is available for this behavior. Bond lengths involving the same atoms increase with the coordination number of E, whether in ionic or extended covalent lattices or molecular compounds. This correlation is sufficiently consistent to use in establishing the coordination number in doubtful cases. Increasing the tin coordination number by one unit, for example, increases tin–ligand distances by ca. 0.1 Å. However, a change from two to three coordination can be much greater (ca. 0.20 for Sn–F, 0.15 for Sn–O, and 0.13 Å for Sn–N).

In descending the fourth group, at germanium and lead is seen the effect of the introduction of an inner shell of, respectively, 10 and 14 electrons residing in rather diffuse orbitals, to produce ${}_{32}\text{Ge}[\text{Ar}]-3d^{10}4s^24p^2$ and ${}_{82}\text{Pb}[\text{Xe}]4f^{14}5d^{10}6s^26p^2$. There is as a consequence a rise in ionization potential and a shrinkage in size of these elements in comparison with their immediate congeners.

As the electronegativity of the E atom increases, the electron pair shared by the E(II) atom will be more contracted. Thus, the space occupied will be less. Bonds adjacent to lone pairs should experience the largest repulsions and become longer than those farther away. While long bonds are usually trans to each other, short bonds are usually trans to a vacancy in the coordination sphere. We infer the position of the lone pair from the nature of these geometric distortions.

Neither the force law governing the repulsions of lone and bonding electron pairs between themselves and each other, nor the precise nature of the force, is known. The ratio of the lone pair–lone pair/bonding pair–bonding pair repulsions is also unknown. The details of this potential, especially the hardness of the pair repulsion law, which might be expressed as the magnitude of n in $\sum r_{ij}^{-n}$ where r is a distance parameter, varies with the individual system.

In analyzing the available data we have adopted an *inclusive* position with respect to coordination number; that is, if the distance to a neighboring atom is within van der Waals radii sums, or the atom is in a suggestive stereochemical position, then it will be regarded by us to be within the coordination sphere. Thus, although we take note of the arguments presented by the original authors, we may raise many of their assigned coordination numbers.

Distortions in molecular solids seem to reflect a compromise between optimal packing or lattice energy, on the one hand, and optimal shape for the molecule, on the other. Deformations follow paths of least resistance which can be discerned theoretically from molecular orbital (MO) studies, semitheoretically from electrostatic or nonbonding models, or empirically from force constants associated with internal vibrations.

When ligand—ligand distances lessen to the sum of their normal van der Waals radii, repulsive forces may begin to override the stereochemical influence of the lone pair. In addition, the stronger (shorter) are the same as bonds holding the ligands, the larger are the angles between them. Ligand–ligand repulsions are greater when the ligands are either tightly bound or sterically demanding. Thus, high-symmetry environments in E(II) compounds should tend to be found in their heavier halide and chalcogenide derivatives and where these anions are in close contact. Repulsions between the bonding electrons may also be important.

The geometric arrangements resulting from five and seven or more electron pairs are not immediately obvious, and in these cases the actual result depends upon the precise details of the potential invoked between the charges. Such systems with large numbers of electrons are usually flexible, with several arrangements close in energy.

The Lewis acidity of E(II) derivatives is characteristic; the Lewis basicity (42, 43, 69), on the other hand, has proved difficult to demonstrate conclusively.² Basicity involving the lone-pair electrons should increase with $R_2E(II)$ angles since the lone-pair orbital will acquire more p character as the bonding orbitals become more s .

No examples of the bare E^{2+} cation exist in any of the structures studied thus far. Neither does the RE^+ cation appear, except in $\eta^5-(CH_3)_5C_5Sn^+BF_4^-$ (91, 92), $\eta^5-(CH_3)_5C_5Sn \cdot bipy^+SO_3CF_3^-$ ($bipy$ = bipyridyl) (99), $\eta^5-(CH_3)_5C_5SnC_5H_5N^+SO_3CF_3^-$ (93), $\{[BF_4]^-[\mu-\eta^5-(C_5H_5)_2Sn]-\mu-\eta^5-C_5H_5Sn^+ \cdot THF\}_n$ (43), and perhaps in $[(\eta^5-C_5H_5)_2Pb]_n$,¹ whose solid-state structure (133) can be regarded as being composed of $[\eta^5-C_5H_5Pb]^+[\mu-C_5H_5]^-$ units. A recent claim for a bare Sn^{2+} ion in $Sn^{2+}(AsF_3)_2(SbF_6^-)_2$ is based on a very high-velocity tin-119m Mössbauer isomer shift (IS), but in the solid state structure the tin(II) atom appears to be coordinated by nine fluorine atoms in a distorted arrangement, thus revealing the presence of the lone pair (46).

² The structure of $[(CH_3)_3CNSn(II)]_4 \cdot 2AlCl_3$ in which Sn(II) functions as a Lewis base has been crystallographically authenticated [Veith, M., and Frank, W., *Angew. Chem., Int. Ed. Engl.* 24, 223 (1985)].

III. History

The idea of lone pairs was originated by W. J. Pope of Cambridge in 1900 who extended the concept of the three-dimensionality of carbon and nitrogen compounds to those of sulfur. His resolution of sulfonium cations $RR'R''S^+$ with three different substituents into optically active enantiomers suggested that these species were tetrahedral with an invisible substituent. The influence of these lone pairs can hardly be detected in transition metal compounds, but the situation is different for post-transition group central atoms such as Ge(II) As(III), Se(IV), and Br(V) with 30 electrons, In(I), Sn(II), Sb(III), Te(IV), I(V), and Xe(VI) with 48 electrons, and Au(-I), Tl(I), Pb(II), and Bi(III) with 80 electrons (90).

Although W. H. Zachariasen of the University of Chicago correctly pointed out in 1932 that central atoms with certain numbers of valence electrons seem to be displaced away from the centers of their respective coordination polyhedra (173), it remained for N. V. Sidgwick and H. M. Powell of Oxford in their 1940 Bakerian Lecture to specify the unshared (inert) pair of electrons as lying at the root of the geometrical distortion (155). This point was further elaborated by R. J. Gillespie and R. Nyholm of University College, London, in a widely read review of inorganic stereochemistry in 1957 (55). It was here that the simple electrostatic model linking geometry with the number of electron pairs in the valence shell was further refined by the recognition that electron pair repulsions in the valence shell decrease in the sequence lone pair-lone pair > lone pair-bonding pair > bonding pair-bonding pair. L. E. Orgel of Cambridge used mixing of *s* and *p* orbitals to account for the influence of lone pairs on the stereochemistry of subvalent lead ions in 1959 (131). R. J. Gillespie of McMaster expounded on the idea of the stereochemical influence of the lone pair in a series of articles beginning in 1960 (52-54), but D. S. Urch of Queen Mary College, London, pointed out in 1964 that exceptions to this influence could be found among octahedral hexahalo anions of groups V-VII, in which the lone pair is accommodated in an A_{1g} antibonding molecular orbital (165).

Examples of authenticated structures which exhibit stereochemically inert lone-pair electrons (21) lying beyond the scope of this review include the linear Li_2O ; the trigonal-planar Si_3N systems in trisilylamine, $(H_3Si)_3N$, and $\beta-Si_3N_4$, and the carbon atoms in the carbanions $C(CN)_3^-$ and $C(NO_3)_3^-$; the square-planar P(III) porphyrin; the octahedral $SbCl_6^{3-}$, $SbBr_6^{3-}$, SbI_6^{3-} , $BiCl_6^{3-}$, $[BiBr_4]_n^{n-}$, $[BiBr_5]_n^{n-}$, $SeCl_6^{2-}$, $SeBr_6^{2-}$, $SeCl_4py_2$, $TeCl_6^{2-}$, $[TeCl_5]_n^{n-}$, $TeBr_6^{2-}$, TeI_6^{2-} ,

$\text{TeCl}_4 \cdot 2\text{SC}(\text{NMe}_2)_2$, $\text{TeBr}_4 \cdot 2\text{SC}(\text{NMe}_2)_2$; and the square-antiprismatic Cs_2XeF_8 , which adopts a geometry characteristic of a species with one fewer electron pair at the xenon atom (eight rather than nine). Another area of exceptions involves the gauche conformations adopted by molecules with adjacent atoms each holding a lone pair. Hydrazine, for example, in its lowest energy conformation places its lone-pair electrons gauche rather than in the expected anti conformation. However, at least for the hexachloro- and bromotellurate(IV)s, the lone-pair electrons are not spectroscopically inert, because relatively low energy transitions are observed in the electronic spectra involving them, implying delocalization to the halide ligands (32). In addition, TeCl_6^{2-} provides a considerably larger cubic unit cell parameter than SnCl_6^{2-} .

More recent models treat the lone pairs as a ligand (54, 147) or as a dibasic anion (19), or even as possibly residing at a site remote in the lattice (65)! The valence-shell electron-pair repulsion (VSEPR) model developed by Gillespie (52-54) has come under criticism as a teaching device (44) because nonbonded atoms often exert a governing influence on geometry (12); because in simple, small, approximately tetrahedral molecules the bond angles do not decrease as the number of lone-pair electrons on the central atom increases (147); because the magnitudes of the total angular space requirements of the bond and lone pairs of electrons, which vary from situation to situation, must be known before molecular geometries can be predicted (147); because lone-pair electrons are seldom purely derived from single atoms alone, but instead usually contain considerable bonding and hybrid character (154); because more examples of stereochemically inactive lone pairs (Y) are known for AX_6Y systems than examples in which they are active (171); because the so-called "Pauli force" which is supposed to keep electrons of like spin separated in space, and lies at the basis of the VSEPR model, is a fiction (17); and because of the ambiguity concerning whether the basis for the VSEPR rules is electrostatic at all (18). The VSEPR model cannot be applied to transition-metal derivations.

For systems which possess stereochemically active lone-pair electrons in the crystalline state, a definitive experimental answer to the title question is at least in principle available from difference density analysis of X-ray results where the potential for deriving electron distributions from elastic diffraction data is now being realized (13, 31, 104). In one application to subvalent molecules (164), $(\text{CH}_3)_2\text{TeCl}_2$ was shown to possess a peak of $0.27 \text{ e}/\text{\AA}^3$ centered at 0.9 \AA from the Te(IV) atom in the position expected for a lone pair of electrons (175).

IV. Symmetrical Subvalent Systems

A. MOLECULAR

1. *The Divalent Hydrides and Halides*

The simplest divalent main group-four molecule is methylene, $:\text{CH}_2$. Methylene is a three-atom system with six valence electrons that can be bent or linear. In accordance with both the Aufbau and Pauli Principles, four valence electrons are in the C—H bonds, leaving two nonbonded electrons. If these go into separate p orbitals on the carbon atom with their spins parallel, a triplet state is the result. An energy advantage in this arrangement derives from the larger average separation of the two electrons relative to the spin-paired arrangement in the singlet state.

For methylene the ground state has been found experimentally to be the triplet with the singlet state a low-lying neighbor. The triplet and singlet energies and the gap between them vary as the groups attached to the carbon atom are changed (47). However, in both the singlet and triplet states, the CH_2 system is bent ($\angle \text{H—C—H} = 103$ and 133.84° , respectively) (56).

On the other hand, the cyanomethylene $\text{H—}\ddot{\text{C}}\text{—C}\equiv\text{N}$ triplet as well as a number of odd alternant methylene compounds, propargylene and its homologues, $\text{H—}\ddot{\text{C}}\text{—C}\equiv\text{CR}$ ($\text{R} = \text{H}, \text{CH}_3, \text{C}_6\text{H}_5$), and $\text{H—}\ddot{\text{C}}\text{—C}\equiv\text{CC}\equiv\text{CR}$ [$\text{R} = \text{CH}_3, \text{C}(\text{CH}_3)_3, \text{C}_6\text{H}_5$] have been predicted to be linear on the basis of the zero-field splitting parameters from electron spin resonance (ESR) experiments (15). The linear nature of the first named $\text{H—}\ddot{\text{C}}\text{—C}\equiv\text{N}$ triplet carbene has been confirmed by a microwave study in the gas phase. However, if the potential well in which the linear configuration lies is shallow, the ground state may not show the effects of nonlinearity (142).

All techniques employed agree that the divalent hydrides and halides of silicon to lead are nonlinear in all phases (22, 74, 84, 105, 125, 153).

2. $[\eta^5\text{-C}_5\text{H}_5\text{Mn}(\text{CO})_2]_2\text{Ge}$

Acetic acid treatment of the transition metal Ge(IV) hydride salt $\text{K}[\eta^5\text{-C}_5\text{H}_5\text{Mn}(\text{CO})_2\text{GeH}_3]$ yields a red product, $[\eta^5\text{-C}_5\text{H}_5\text{Mn}(\text{CO})_2]_2\text{Ge}$, which contains a linear Mn—Ge—Mn system in which the germanium atom occupies a special position with equal Ge—Mn distances of 2.204 Å. Solution infrared spectra show four $\nu(\text{CO})$ stretching absorptions instead of the two expected from the centrosymmetric structure in the solid state, implying free rotation about the Ge—Mn bonds. Simple application of the rare-gas rule would favor a double-bonded formulation containing Ge(IV), but a molecular-orbital

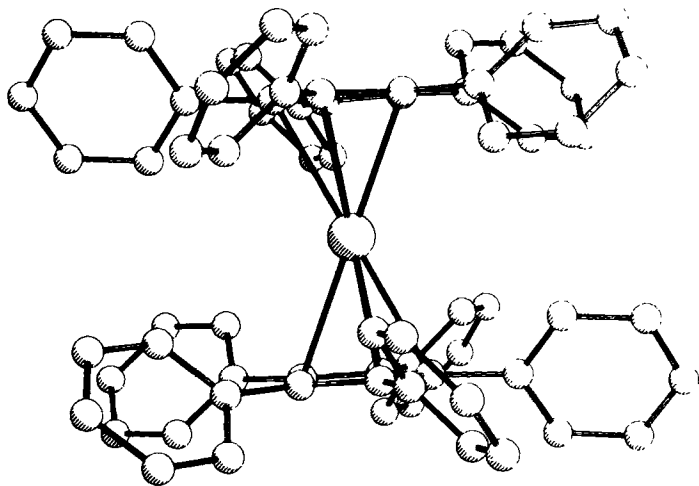


FIG. 1. Decaphenylstannocene, $[\eta^5\text{-(C}_6\text{H}_5)_5\text{C}_5\text{]}_2\text{Sn}$, viewed parallel to the plane of the cyclopentadiene rings (from ref. 77).

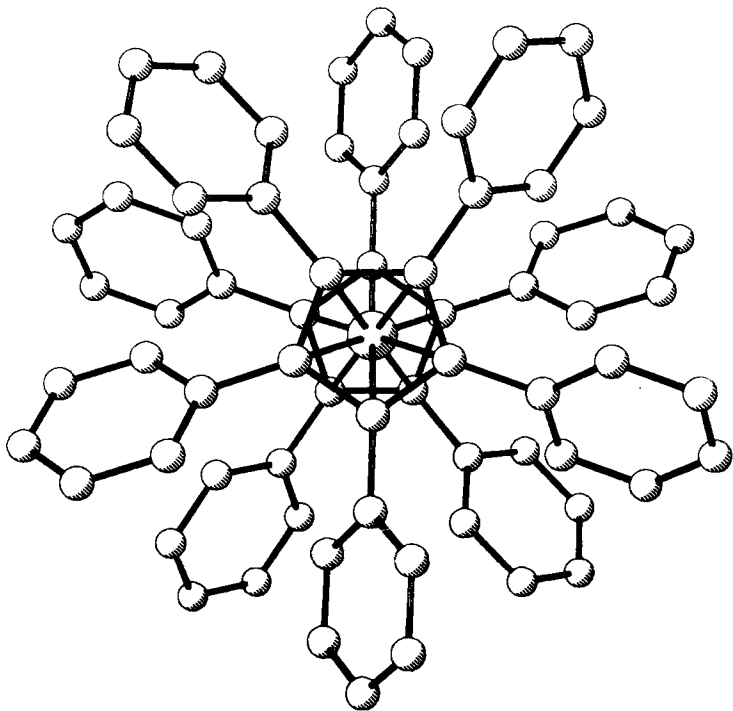


FIG. 2. Decaphenylstannocene, $[\eta^5\text{-(C}_6\text{H}_5)_5\text{C}_5\text{]}_2\text{Sn}$, viewed perpendicular to the plane of the cyclopentadienyl rings (from ref. 77).

calculation suggests partial three-center bonding in agreement with the rather free rotation found. The short Ge–Mn bonds favor the multiple-bond description (110).

3. $[\eta^5\text{-(C}_6\text{H}_5)_5\text{C}_5]_2\text{Sn}$

Decaphenylstannocene is the only molecule to occupy the S_{10} symmetry class. The tin atom sits on an inversion center between symmetry-related, equidistant [2.401 Å to the ring centers; $d(\text{Sn}-\text{C}_{\text{ring}}) = 2.692$ Å (av.)] cyclopentadienes that are perfectly planar, perfectly staggered, and exactly parallel (see Figs. 1 and 2). The attached phenyl groups are canted to each cyclopentadienyl ring oppositely in an opposed paddle wheel fashion. There are no short intermolecular contacts in the solid (see Fig. 3) (7, 8, 77).

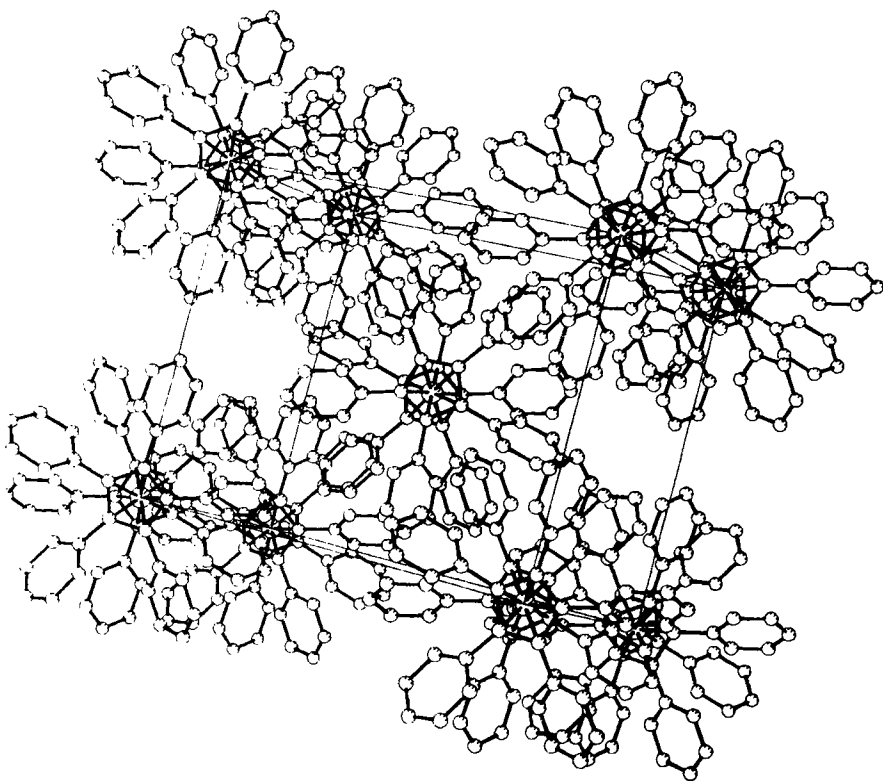


FIG. 3. Packing diagram of decaphenylstannocene, $[\eta^5\text{-(C}_6\text{H}_5)_5\text{C}_5]_2\text{Sn}$ (from ref. 77).

The fortuitous formation of η^5 -pentaphenylcyclopentadienyl derivatives of the transition metals under mild reaction conditions is evidence for the stabilizing power of that ligand. Aside from imparting high kinetic stability through its large volume, electron withdrawal by the phenyl groups makes low oxidation states of the transition metals more accessible. Since the tin(II) $5s^2$ electrons are not occupying their usual nonbonding orbital, and all the bonding orbitals are filled, then these electrons must occupy an orbital with antibonding character. The phenyl rings, which are not antiparallel to the cyclopentadiene rings, can help to delocalize these electrons. The germanium and lead derivatives are also available (88). The tin-119m Mössbauer spectrum of decaphenylstannocene is unremarkable (38, 88, 140, 177, 178) for a structurally authenticated (38, 157, 176) stannocene or its derivatives (42, 68, 69).

Pentaphenylstannocene, $\eta^5\text{-(C}_6\text{H}_5)_5\text{C}_5\text{Sn(II)C}_5\text{H}_5\text{-}\eta^5$, is bent, although some charge delocalization is possible because the five attached phenyl groups are not perpendicular to their cyclopentadiene ring (27). The decabenzylmetallocenes, $[\eta^5\text{-(C}_6\text{H}_5\text{CH}_2)_5\text{C}_5]_2\text{E(II)}$ (E = Ge, Sn, Pb), are also bent (27, 151a, 151b).

B. EXTENDED LATTICES

1. Germanium

a. GeCl_3^- Salts. In the salts of GeCl_3^- with Rb^+ (111), Cs^+ (28), $[\text{N}(\text{CH}_3)_4]^+$ (35), and $[\text{NH}(\text{CH}_3)_3]^+$ (114), as well as the pilocarpine ($\text{C}_{11}\text{H}_{17}\text{N}_2\text{O}_2$) hemihydrate (49), the germanium atom occupies a site with three short and three long Ge-Cl distances to give a distorted octahedron with two very different opposite triangular faces showing the structure-distorting effect of the lone-pair electrons. However, CsGeCl_3 undergoes a transition at 155°C as shown by differential thermal analysis (DTA) from its rhombohedrally distorted perovskite lattice to a cubic high-temperature phase (space group $Pm\bar{3}m$), and this transition is accompanied by a discontinuity in specific electrical conductance. The dielectric constant (1500 at 25°C) rises to 5800 at 155°C and then falls (28). The $[\text{N}(\text{CH}_3)_4]^+$ salt also undergoes a phase transition from space group $Pna2$ to an anionic, conducting cubic phase at 151°C (space group $Pm\bar{3}m$) (35). The room-temperature electrical conductivity of 10^{-8} increases to $10^{-2} \Omega^{-1} \text{ cm}^{-1}$, and the lattice constants expand by *ca.* 20%. The heat of transformation (115) is 3.1 kJ mol^{-1} , but the thermal stability range of the cubic phase is quite narrow since decomposition occurs at 22°C above the transition point (35).

b. Germanium Monochalcogenides. The orthorhombic GeS (157*a*, 170, 173) and GeSe (45, 87, 95, 130, 149, 157*a*, 173) compounds display anomalies of thermal expansion in the range 230–500 and 400–500°C, respectively; GeSe transforms in one step at 651°C to the rock-salt structure, and GeS melts at 658°C before a potential transition to the NaCl structure can take place. For GeTe, the rhombohedral, face-centered lattice (57, 150, 174) is converted in a first-order phase transition to the NaCl structure (16) at 300°C, accompanied by a shrinkage in volume of 1.4% (174).

c. GeBi₂Te₄. Electron diffraction (at the $R = 23\%$ level) of a hexagonal film of GeBi₂Te₄ (space group $R\bar{3}m$) on NaCl reveals the germanium atoms lying on octahedral sites symmetrically surrounded by six tellurium atoms (3).

d. Ge₃Bi₂Te₆. Electron diffraction (at the $R = 19.6\%$ level) of a hexagonal film of Ge₃Bi₂Te₆ (space group $R3m$) on NaCl gives a closest packed cubic arrangement of germanium atoms in octahedral sites symmetrically surrounded by six tellurium atoms (134).

e. K₂Ge₂O₃. The oxogermanate(II), K₂Ge₂O₃, has a body-centered cubic structure from X-ray powder data. Annealing at 380°C for 1 week produces no changes (81).

2. Tin

a. CsSnCl₃. Monoclinic (136) [or triclinic (20)] white CsSnCl₃ (space group $P2_1/n$, m.p. 383°C) undergoes an irreversible phase transition at 117°C to a bright yellow, ideal cubic perovskite (11, 138, 146). While the low-temperature form exhibits a tin-119m Mössbauer QS of 0.90 mm sec⁻¹, the cubic form has a single, sharp line with no resolvable QS, consistent with the tin atoms being located at a cubic site (11). In addition, the low-temperature form exhibits three chlorine-35 NQR resonances of equal intensity, consistent with three inequivalent chlorine atom sites in the pyramidal SnCl₃⁻ anion. Unfortunately, the resonance in the cubic form could not be observed (146). Both the high- and low-temperature forms are electrical insulators (146). The cell length reported previously (136) has been determined to be erroneously too small (11).

b. CsSnBr₃. Black CsSnBr₃ exhibits metallic luster and is cubic (11) (space group $Pm\bar{3}m$) at room temperature ($R = 11\%$) (41). The conductivity is 0.05 Ω⁻¹ cm⁻¹ at ambient temperature and shows metallic-type behavior between 100 and 350°C with no major change in conductance observed. The material turns dark red between 350 and 400°C and melts to a clear, dark-red liquid at 450°C. The color changes

reverse upon cooling (146). The conductivity and color behavior reported (11) are said to correspond to the material treated in air (146). There is no resolvable QS in the tin-119m Mössbauer spectrum, consistent with the tin atoms occupying sites of cubic symmetry at the center of a regular octahedron of bromine atoms (11, 39–41). At 12°C, some weak extra X-ray powder lines appear, and a transformation to a lower symmetry form is corroborated by bromine-81 NQR and DTA data. However, a single NQR resonance is observed in the range 19.6–100°C (146).

c. $[\text{CH}_3\text{NH}_3]^+\text{SnBr}_3^-$. This compound crystallizes in a perovskite structure with the tin(II) atom in octahedral coordination (108).

d. CsSnI_3 . Yellow, orthorhombic CsSnI_3 (m.p. 452°C) crystallizes in needle form (space group $Pnam$) with the tin(II) atoms at the center of a distorted octahedron of iodine atoms (107). The yellow material begins to darken above 100°C, and at 152°C transforms to a shiny black, cubic perovskite form which is an electrical conductor (conductivity at room temperature is $0.04 \Omega^{-1} \text{ cm}^{-1}$). Between 350 and 400°C it turns slightly dark red. The melt is black and opaque, and the vapor yellow. Upon solidification, CsSnI_3 remains black when cooled to room temperature. Unfortunately, no iodine-127 NQR signals could be found for the black, cubic form, but the yellow monoclinic form gives a single line whose frequency decreases approximately linearly with increasing temperature from 35 to 105°C (146).

e. $[\text{CH}_3\text{NH}_3]^+\text{SnBr}_x\text{I}^{3-x}_3$ ($x = 0-3$). These intensely colored, electrically conducting compounds exhibit cubic perovskite structures on the basis of X-ray powder data, with the tin(II) atoms at the center of octahedra formed by the halogen atoms. The data can be indexed in terms of a primitive cubic lattice. For the anthracite-colored $[\text{CH}_3\text{NH}_3]^+\text{SnI}_3$, the $Pm3m$ space group can be assigned. For this compound there are no resolvable tin-119m Mössbauer QS at 85 or 298 K, and none at 298 K for the wine-red SnBr_3^- analogue. Both the latter and the black SnBr_2I^- derivative show small QS values at 85 K. At 290–300°C, the SnBr_3^- and SnI_3^- salts melt to light yellow and blue-black liquids, respectively, with decomposition to a vapor, presumably containing $\text{CH}_3\text{NH}_3\text{Br}$ and $\text{CH}_3\text{NH}_3\text{I}$. The electrical conductivity maximizes with the SnI_3^- derivative (169).

f. $[(\text{C}_2\text{H}_5)_4\text{N}]^+\text{SnI}_3^-$. The tin(II) atom here occupies an octahedral site surrounded by six iodine atoms. Linear, one-dimensional chains of tin atoms parallel to the c -axis are bridged by iodine atoms (108).

g. Cs_4SnBr_6 . The white, ambient-temperature form turns black on heating or when prepared from the molten CsBr-SnBr_2 system. X-Ray powder data for the black form suggest a hexagonal structure (41) similar to that of Cs_4PbBr_6 , which contains discrete $[\text{PbBr}_6]^{4-}$ anions (118). The tin-119m Mössbauer resonance is a narrow singlet at 4.2 K, consistent with a high-symmetry $[\text{SnBr}_6]^{4-}$ environment (41). This regular octahedral geometry has been confirmed by an unpublished single-crystal X-ray study (6).

h. SnTe . Both the ambient α (170) and high-temperature (β) forms (168) of SnS and SnSe (157a) are orthorhombic, with space groups $Pbnm$ for the former and $Cmcm$ for the latter. Earlier reports of cubic phases (132, 141) or films (112, 113) are in error (9).

Cubic SnTe has an NaCl structure at room temperature with two interpenetrating face-centered cubic sublattices formed by tin(II) and tellurium atoms (1, 2, 72, 73, 126, 128). The cubic form undergoes a transition to a rhombohedral structure at temperatures below 5 K (16, 123) and to an orthorhombic one (space group $Pnma$) at 18 kbar (94).

i. SnI_2 . Brilliant red tin(II) iodide crystallizes in the monoclinic space group $C2/m$ as needles which contains two distinct tin sites, one of seven coordination occupied by two-thirds of the tin atoms, and one of six coordination occupied by the rest (121). The former is of distorted geometry with tin-iodine distances suggestive of a primary trigonal pyramid in a trigonal prism with an additional nearest neighbor. In the latter the tin atom lies on a center of symmetry and is surrounded octahedrally by iodine atoms (82). The monoclinic crystals have also been described as transparent bright yellow from growth in silica gel (36). The tin-119m Mössbauer spectrum fails to reveal the true complexity of the structure. The two tin sites apparently have quite similar IS, and the seven-coordinated site exhibits only a weak QS (82).

j. $[\text{Rh}(\text{NH}_3)_6]_3^{3+}[\text{Rh}(\text{SnCl}_3)_4\text{SnCl}_4]^{5-}[\text{SnCl}_6]^{4-} \cdot 4\text{H}_2\text{O}$. This violet, extremely polychroic salt consisting of three $[\text{Rh}(\text{NH}_3)_6]^{3+}$ cations, two kinds of anions, $[\text{Rh}(\text{SnCl}_3)_4\text{SnCl}_4]^{5-}$ and $[\text{SnCl}_6]^{4-}$, and four waters of crystallization forms in the monoclinic space group $P2/n$. The tin(II) atom in the hexachlorostannate(II) dianion lies on a twofold axis with Sn-Cl distances ranging from 2.7631 to 2.8942 Å, and Cl-Sn-Cl angles of 84.29, 95.96, and 175.83° (97). Tin-119m Mössbauer data show the presence of this tin(II) atom (96, 144). While the unique tin(II) atom is at the center of a slightly less-than-perfect octahedron of chlorine atoms, the extremely long Sn-Cl bonds (97) signal the stereochemical inertness of the lone-pair electrons, and hence this compound is included here.

3. Lead

a. PbF_2 . Orthorhombic $\alpha\text{-PbF}_2$ (145) (space group $Pmnb$) undergoes a phase transition at 315°C to a cubic β form (154) (space group $Fm3m$) (172), accompanied by a lattice expansion. The anions and cations coordinate one another in the form of regular cubes and regular tetrahedra, respectively. Thus the Pb(II) atoms are eight coordinated with the fluorine atoms located at the corners of a regular cube, and each fluorine atom is surrounded by four metal atoms at the corners of a regular tetrahedron. This fluorite-structure material exhibits high ionic conductivity ($1\ \Omega^{-1}\text{ cm}^{-1}$) at high temperatures (ca. 425°C) (152). At lower temperatures the ionic conduction is carried mainly by extrinsic defects which can be generated by doping $\beta\text{-PbF}_2$ with either divalent anions (e.g., O^{2-}) or mono- or trivalent cations (e.g., Ag^+ , La^{3+}). At higher temperatures the ionic conduction is carried by intrinsic defects (10, 37, 86, 101).

b. PbI_2 . Yellow PbI_2 (m.p. 400°C) has the CdI_2 hexagonal layer lattice structure (163, 166). The material is a photoconductor and decomposes on exposure to green light ($\lambda = 494.9\text{ nm}$). The lead atoms are in alternate layers of octahedral sites sandwiched between layers of iodine atoms. Organic donor molecules can intercalate into the layer lattice, which retains its hexagonal symmetry (100).

c. CsPbF_3 . At 615°C CsPbF_3 transforms into a primitive cubic perovskite lattice. The lower-temperature β form also has a perovskite lattice, but with a tetragonal distortion (148). The melting point is 725°C .

d. CsPbCl_3 . The pale-yellow rectangular crystals (109) of CsPbCl_3 undergo three successive phase transformations: at 37°C , from monoclinic to orthorhombic; at 42°C , from orthorhombic to tetragonal; and at 46.9°C , from tetragonal to cubic (50, 117, 119, 129). The structure of the high-temperature form is not entirely straightforward since single-crystal neutron diffraction data (at the $R = 9\%$ level) at 55°C can be interpreted in terms of a cubic perovskite structure with anisotropic thermal vibration, or a disordered structure with several potential minima for the cesium and chlorine atoms (66). X-Ray powder data can be interpreted in terms of distortions from the ideal cubic structure arising from various tilts of the PbCl_6 octahedra about one or more of the cubic faces (4). The anharmonicity in cubic CsPbCl_3 is quite marked (50), and the cubic to tetragonal transition is discontinuous (83), with the PbCl_6 octahedra oscillating in phase along a particular direction (50). In addition, there may be competing instabilities in the cubic phase

(83). Disordered models for the chlorine atoms are not currently favored (66, 83), but the origin of the lead atom anharmonicity cannot be said to be settled yet (83, 124a). The lower temperature phases may be better understood (25, 80).

e. $[\text{CH}_3\text{NH}_3]^+\text{PbX}_3^-$ ($\text{X} = \text{Cl}, \text{Br}, \text{I}$). These three compounds have the cubic perovskite structure. With the exception of the colorless chloride, they show intense color (red-orange for the bromide and black for the iodide). However, there is no significant conductivity under normal conditions. The mixed halides have intermediate colors. Decomposition occurs at ca. 300°C without melting, but they are far more stable to oxidation than the corresponding tin(II) analogues (see Sections IV, B, 2, c and IV, B, 2, e, above). Apparently, the nonspherically symmetrical methylammonium cation does not encroach upon the octahedral symmetry of the lead halide system (169).

f. CsPbBr_3 . The white, low-temperature form of CsPbBr_3 is orthorhombic (space group $Pmnb$) (106) and contains distorted PbBr_6 octahedra. Above 130°C , however, a cubic perovskite structure forms (119, 120). This material behaves like the analogous chloride, whose structure is discussed in Section IV, B, 3, d, in that there are anisotropic thermal vibrations and anomalously large thermal parameters for the cesium and bromine atoms (143).

g. MPbI_3 ($\text{M} = \text{Rb}, \text{Cs}, \text{R}_4\text{N}^+$). Yellow, orthorhombic CsPbI_3 (space group $Pmnb$) contains distorted PbI_6 octahedra. On heating these crystals to $305\text{--}308^\circ\text{C}$, they undergo a phase change to an unstable, black, monoclinically distorted perovskite structure (116). The material is photoconductive, having its maximum spectral sensitivity in the red region, the one complementary to the color of the crystal (120).

The isomorphous rubidium analogue crystallizes in the orthorhombic space group $Pnam$. Again, the PbI_6 octahedra are not precisely ideal. The lead-iodine internuclear distances are in the range $3.037\text{--}3.382 \text{ \AA}$ (76).

Tetramethylammonium triiodolead(II), $[(\text{CH}_3)_4\text{N}]^+\text{PbI}_3^-$, is hexagonal (space group $P6_3/m$) with octahedrally coordinated Pb(II) atoms. The $(\text{CH}_3)_4\text{N}^+$ cations are disordered. Two unique angles, 86.25 and 93.75° , characterize the lead atom site which has crystallographic $\bar{3}$ point symmetry. The octahedron is stretched along one axis. The lead-iodine internuclear distance is 3.223 \AA (30).

The hydrates $\text{KPbI}_3 \cdot 2\text{H}_2\text{O}$, $\text{NH}_4\text{PbI}_3 \cdot 2\text{H}_2\text{O}$, and $\text{RbPbI}_3 \cdot 2\text{H}_2\text{O}$ are isostructural, crystallizing in the space group $Pnma$. The PbI_6 octahedra are distorted. The lead-iodine internuclear distances range from 3.03 to 3.46 \AA (14).

Thus, while all the PbI_6 octahedra in these structures are distorted, the materials are included here for completeness.

h. PbS. Lead(II) sulfide (m.p. 1112°C), which crystallizes with the NaCl structure (23), is opaque and possesses a brilliant metallic luster as the black mineral galena. This is the principal ore of lead and its only sulfide. The pure material is an intrinsic semiconductor, which, in the presence of impurities or in stoichiometric imbalance, can develop either n- or p-type semiconductor properties. It is also a photoconductor, and is one of the most sensitive detectors of infrared radiation. The photovoltaic effect in this material is the basis for its use in photographic exposure meters.

The charge distribution in the cubic PbS rock-salt structure (6:6 coordination; space group $Fm\bar{3}m$) has been studied at ambient temperature by X-ray diffraction at the $R = 1.5\%$ level. The direct integration of charge density, the observed atomic scattering factors, and the population analysis of the valence electrons all indicate that the lead atom is negatively charged, i.e., electrons are transferred from sulfur to lead. No overlap density was observed in the deformation density map. Thus the bonding electrons in this crystal may be delocalized like free electrons in metals. The thermal parameters of the lead atoms are larger than those of the chalcogens. Anharmonic thermal vibration of the lead atom is detected in the difference electron density map (127).

i. PbSe. The three lead(II) chalcogenides (137), PbS, PbSe, and PbTe, are unusual in that their color diminishes with increasing mass of the chalcogen. Lead(II) sulfide (see Section IV, B, 3, *h*) is black, the selenide is grey, and PbTe (see Section IV, B, 3, *j*) is white. All three materials possess the cubic rock-salt structure (space group $Fm\bar{3}m$); all three are photoconductors.

Lead(II) selenide, (m.p. 1075°C), found as the mineral Clausthalite, has been studied by X-ray diffraction at the $R = 1.1\%$ level. The results of this study are the same as those described in Section IV, B, 3, *h* for PbS, except that the ratio of thermal parameters for lead vs. the chalcogen is even larger in PbSe (127).

j. PbTe. Lead(II) telluride (m.p. 917°C) occurs naturally as the mineral Altaite, but can be made directly by heating stoichiometric amounts of the elements. The product is a white material which crystallizes in the cubic rock-salt structure (space group $Fm\bar{3}m$). Study by X-ray diffraction at the $R = 1.5\%$ level yields results similar to those discussed for PbS in Section IV, B, 3, *h*, except that here the ratio of the thermal parameters for lead vs. the chalcogen is even greater than for PbS or PbSe. A valence electron population analysis gives effective

charges at the lead atom of -1.2 , -0.9 , and -2.7 for PbS, PbSe, and PbTe, respectively (see Sections IV, B, 3, h and IV, B, 3, i) (127, 157a).

k. Lead(II) Thiourea Complexes. Thio- and selenoureas can serve as precursors in the synthesis of the Pb(II) chalcogenides described above. The thiourea complexes of Pb(II) show many different compositions and structural types (58–64, 78, 79), which include six- and eightfold coordination of the lead(II) atoms by sulfur. While in no case reported thus far has the lead(II) atom been found at a site of perfect symmetry, the following two compounds are included here because in each one there is a lead(II) atom at the center of a polyhedron which is only slightly distorted.

(1) $\frac{3}{4}\text{Pb}(\text{HCO}_2)_2 \cdot 4\text{SC}(\text{NH}_2)_2$. The title compound, unlike several analogues, is fully ordered and has one lead(II) atom in a symmetrical, eight-coordinated site. The structure consists of infinite polymeric chains, but with every fourth lead position along the chain vacant. These ordered vacancies account for the unusual stoichiometry. The material precipitates from saturated greenish-yellow aqueous formic acid solutions of Pb(II) formate and thiourea as white needles (space group *I422*). The structural motif consists of three lead atoms in twisted trigonal prisms (twist angle $\sim 28^\circ$) formed by the sulfur atoms of the thiourea molecules. One lead atom is at the center of gravity (not a center of symmetry) of the central prism. Successive motifs along a lead–thiourea chain are separated by empty prisms. The distances between successive squares of sulfur atoms (these four sulfur atoms are related by a fourfold axis and hence lie in one plane) are equal whether the prism is occupied by a lead atom or not. The central Pb(II) atom is symmetrically situated at long but equal distances from the surrounding sulfur atoms (see Figs. 4–6) (59).

(2) $\text{Pb}[\text{SC}(\text{NH}_2)_2]_6^+ [\text{ClO}_4]_2^-$. White, triclinic needles (space group *P1*) precipitate from saturated aqueous thiourea to which stoichiometric $\text{Pb}(\text{ClO}_4)_2$ has been added (1:6). The lead(II) atom lies at the origin of the unit cell, equidistant from six sulfur atoms at the center of a slightly distorted octahedron characterized by three independent angles ($\bar{1}$ symmetry) ranging from 79 to 100° (see Fig. 7) (58).

l. $\text{M}_2\text{PbCo}(\text{NO}_2)_6$ ($\text{M} = \text{Rb}, \text{Cs}$). The $\text{M} = \text{Rb}$ and Cs materials crystallize in cubic phases (24, 48) (space group *Fm3*) containing both $\text{Co}(\text{NO}_2)_6$ and Pb(II) groups with *m3* symmetry (103). A wide range of hexanitrito complexes of the first-row transition metal ions are known (74a), and many have been shown to take face-centered cubic structures. The presence of the lead(II) ion may contribute to the stabilization of

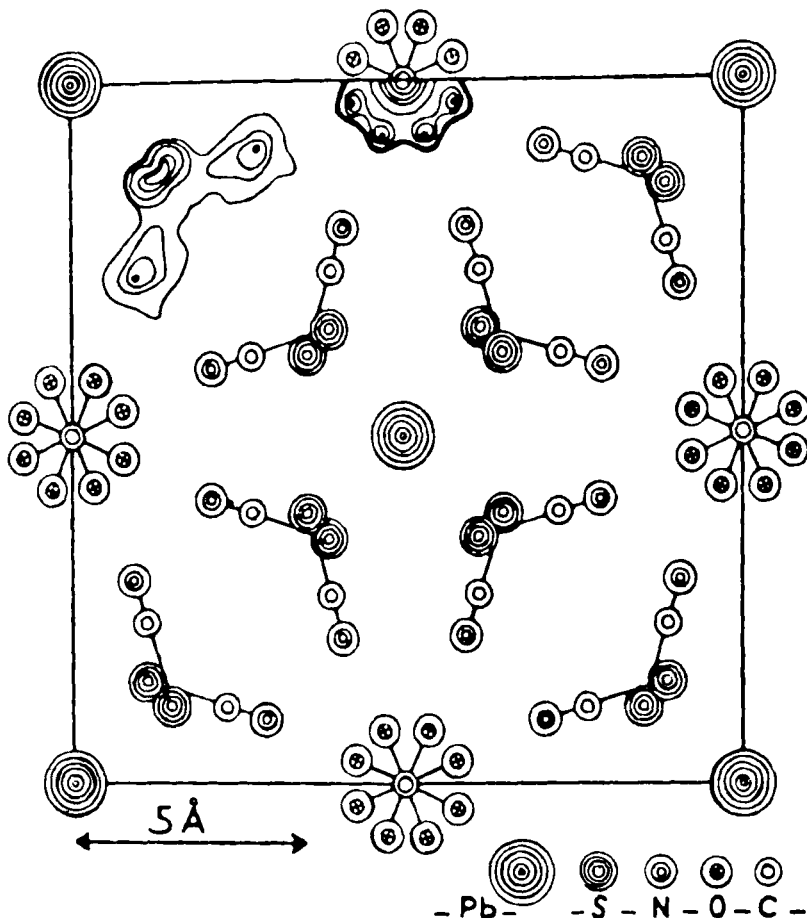


FIG. 4. The structure of $\frac{3}{4}\text{Pb}(\text{HCO}_2)_2 \cdot 4\text{SC}(\text{NH}_2)_2$ in projection down $[001]$ (from ref. 59).

these cubic phrases (48). Powder electron spin resonance (ESR) spectra at 296 K are isotropic as expected. The lead(II) atom is found at the center of 12 nitrite oxygen atoms in a cubic geometry (103).

m. $\text{K}_2\text{PbNi}(\text{NO}_2)_6$. The lead(II) atom is found at the center of a cube formed by the 12 nitrite oxygen atoms in this cubic (space group $Fm\bar{3}$) crystal in which the $\text{Ni}(\text{NO}_2)_6$ groups also have $m\bar{3}$ symmetry. The cubic symmetry is retained down to 130 K unlike the copper homologue (see Section IV,B,3,n), which transforms to an orthorhombic form at 233 K (158, 160). Among the hexanitritonickelates, the lead(II) derivative exhibits different electronic and electron spin resonance (ESR) behavior than, for example, the alkaline-earth analogues (75).

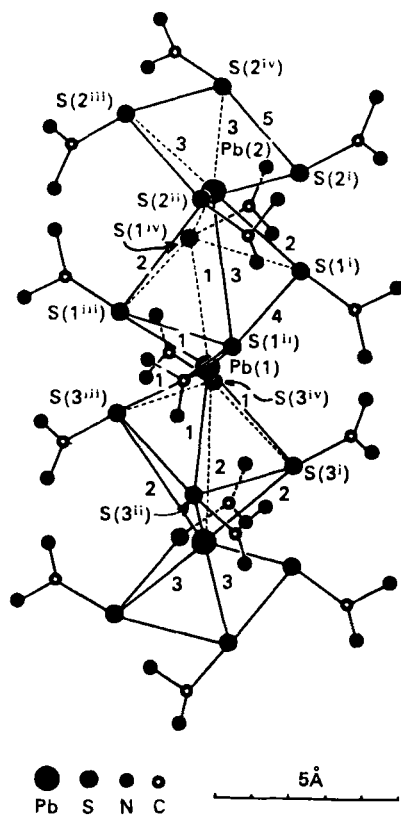


FIG. 5. The structural motif in $\frac{3}{4}\text{Pb}(\text{HCO}_2)_2 \cdot 4\text{SC}(\text{NH}_2)_2$ (from ref. 59).

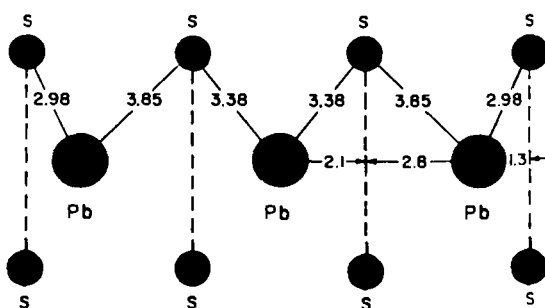


FIG. 6. Internuclear distances in the cation motif in $\frac{3}{4}\text{Pb}(\text{HCO}_2)_2 \cdot 4\text{SC}(\text{NH}_2)_2$ (from ref. 59).

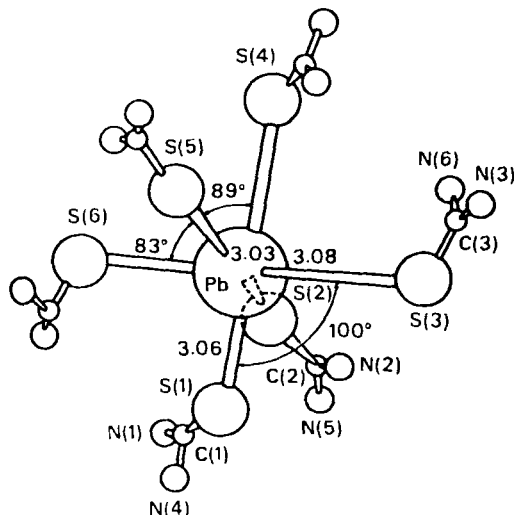


Fig. 7. Geometry of the $\text{Pb}[\text{SC}(\text{NH}_2)_2]_6^{2+}$ cation in the perchlorate salt (from ref. 58).

n. $\text{M}_2\text{PbCu}(\text{NO}_2)_6$ ($\text{M} = \text{K}, \text{Rb}, \text{Cs}, \text{Tl}$). The $\text{M} = \text{K}$ derivative is face-centered cubic (space group $Fm\bar{3}$) with the copper atoms at the centers of regular octahedra and the lead(II) atoms at the centers of perfect cubes (25, 33, 167) (see Fig. 8) (85). Reversible transformations to less symmetrical tetragonal phases occur at 281 and 273 K (48). In the $\text{Cu}(\text{NO}_2)_6^{4-}$ anion the NO_2 groups trans to each other are coplanar and parallel to the axial plane to give T_h symmetry. The electron spin resonance (ESR) spectrum is a single isotropic line at 300 K, but the spectrum at 77 K is anisotropic (71). The cubic $\text{M} = \text{Tl}$ derivative is isomorphous (space group $Fm\bar{3}$) at 295 K and undergoes phase changes at 245 and 241 K, which give rise to changes in the ESR spectra and lattice dimensions (70, 159). The $\text{M} = \text{Rb}$ derivative is orthorhombic (space group $Fmmm$), but transforms to a cubic structure (139) (space group $Fm\bar{3}$) above 317 K (161, 162). The phase transitions in $\text{Cs}_2\text{PbCu}(\text{NO}_2)_6$ take place at 275 and 289 K and at 381 and 391 K (on cooling and heating, respectively). A third transition occurs at 294 and 310 K. The first of these transitions gives an orthorhombic material (space group $Fmmm$). The lead-oxygen distances are in the range 2.849–2.858 Å (124). A second material is monoclinic (space group $B2/b$) (98).

o. Miscellaneous Lead(II) Oxides. The question of the stereochemical activity of the lone-pair electrons in divalent tin and lead oxides has been carefully treated recently (138). No examples of sites of perfect symmetry are available, but the following systems deserve mention.

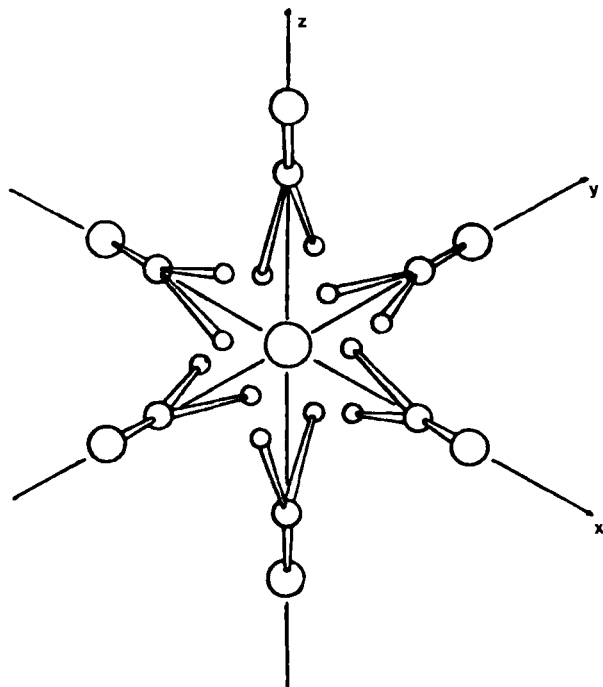


FIG. 8. The arrangement of the nitrito groups about the lead(II) atom in $\text{K}_2\text{PbCu}(\text{NO}_2)_6$ (from ref. 85).

(1) PbWO_4 . Lead(II) tungstate is isostructural with Scheelite, CaWO_4 , whose structure is built up from isolated WO_4 tetrahedra which are connected through PbO_8 polyhedra. The lead(II)–oxygen internuclear distances fall into two groups of four at near 2.645 and 2.670 Å (mean 2.66 Å). These values are comparable with those observed in the strontium (2.49 and 2.59 Å) and barium (2.68 and 2.688 Å) homologues. Thus it appears that the lone-pair electrons at Pb(II) play little role here (135, 156).

(2) PbCrO_4 . The orthorhombic form of lead(II) chromate is also built up from CrO_4 tetrahedra linked through PbO_{12} polyhedra characterized by lead(II)–oxygen distances in the range 2.64–3.57 Å (29).

(3) PbNb_2O_6 . The rhombohedral form of PbNb_2O_6 is only stable at low temperatures, transforming to the tetragonal tungsten-bronze structure at above 100°C. The former is built up from edge- and corner-sharing NbO_6 octahedra forming two kinds of tunnels—large triangular ones, and others which are very distorted hexagonal. Pyramidal

PbO_3^{4-} anions are located in these tunnels. In the ferroelectric tetragonal phase, on the other hand, there are pentagonal and perovskite tunnels. The Nb atoms are displaced inside their octahedra and the Pb atoms likewise inside their polyhedra in the pentagonal tunnels. However, there are other lead(II) atoms in the pentagonal tunnels which, along with all of those in the perovskite tunnels, are characterized by rather long lead-oxygen distances (2.65–2.89 Å) and relatively small displacements inside their polyhedra (102).

(4) *Cubic pyrochlores*, $\text{Pb}_2\text{M}_2\text{O}_7$. All known exactly stoichiometric cubic pyrochlores of tin and lead (possibly excepting the $\text{M} = \text{U}$ material of lead) are rhombohedrally distorted from the ideal $Fd3m$ space group. Nonstoichiometric, usually oxygen-deficient, pyrochlores of the precious metals, M, can be cubic with the cations in a face-centered array. These materials exhibit metallic conductivity and paramagnetism, but some Pb(IV) atoms often occupy the M sites. In the ideal case the lead(II) cation would be eight-coordinated by oxygen atoms in a hexagonal-bipyramidal geometry. However, the value of x in the oxygen-deficient pyrochlores $\text{Pb}_2\text{M}_2\text{O}_{7-x}$ is nearly one ($\text{M} = \text{Ru}, \text{Ir}, \text{Re}, \text{etc.}$). The M cations are found in perfect octahedra (138).

V. Conclusions

We present in Table I a listing of compounds in which subvalent group-four atoms occupy perfectly symmetrical sites. Only two discrete molecular forms are represented, the rest being extended lattices. The inclusion of compounds with highly, but not perfectly, symmetrical sites would have greatly expanded this list (Table I). Some of these materials are mentioned in the text as an encouragement to further research seeking perfect symmetry phases.

Generalization for these materials is difficult because at the present time not all the desired information has been developed for each system. However, a pattern involving the following phenomena begins to emerge from our survey.

1. Certain subvalent, fourth-group compounds undergo single or a series of first-order phase transformations at increasing temperatures from their expected distorted phases to give successively more symmetrical structures;

2. If the material does not melt first, this may include a phase in which the subvalent group-four atom occupies a site of perfect cubic symmetry;

TABLE I

SYMMETRICAL E(II) STRUCTURES

Molecular	
Ge:	$[\eta^5\text{-C}_5\text{H}_5\text{Mn(CO)}_2]_2\text{Ge}$
Sn:	$[\eta^5\text{-(C}_6\text{H}_5)_5\text{C}_5]_2\text{Sn}$
Extended Lattices	
Ge:	MGeCl ₃ (M = Cs ⁺ , Me ₄ N ⁺)
	GeSe at > 651°C
	GeTe at > 300°C
	GeBi ₂ Te ₄ film on NaCl
	Ge ₃ Bi ₂ Te ₆ film on NaCl
	K ₂ Ge ₂ O ₃
Sn:	CsSnCl ₃ at > 117°C
	MSnBr ₃ (M = Cs ⁺ , MeNH ₃ ⁺)
	MSnI ₃ (M = Cs ⁺ at > 152°C, MeNH ₃ ⁺ , Et ₄ N ⁺)
	Cs ₄ SnBr ₆
	SnTe
	SnI ₂
	$[\text{Rh(NH}_3)_6]_3^{3+}[\text{Rh(SnCl}_3)_4\text{SnCl}_4]^{5-}[\text{SnCl}_6]^{4-} \cdot 4\text{H}_2\text{O}$
Pb:	PbF ₂ at > 315°C
	PbI ₂
	CsPbF ₃ at > 615°C
	MPbCl ₃ (M = Cs ⁺ at > 46.9°C, MeNH ₃ ⁺)
	MPbBr ₃ (M = Cs ⁺ at > 130°C, MeNH ₃ ⁺)
	MPbI ₃ (M = Cs ⁺ at > 305°C, MeNH ₃ ⁺)
	PbS
	PbSe
	PbTe
	M ₂ PbCo(NO ₂) ₆ (M = Rb ⁺ , Cs ⁺)
	K ₂ PbNi(NO ₂) ₆
	M ₂ PbCu(NO ₂) ₆ (M = K ⁺ , Rb ⁺ , Cs ⁺ , Tl ⁺)

3. The materials which contain perfectly symmetrical sites for the subvalent fourth-group atom have regular octahedral (six) or cubic (eight-) or dodecahedral (12-coordinated) environments consisting of equidistant halogen (F, Cl, Br, or I) or chalcogen (O, S, Se, or Te) nearest neighbors. In the regular cubic examples only oxygen has been found thus far to be present; all the regular cubic geometries discovered have lead(II) atoms surrounded by 12 oxygen atoms. Examples with asymmetric gegen ions exist, as do examples arising from epitaxial effects on materials deposited on rock-salt surfaces;

4. Evidence for the cubic symmetry can come from the observation of single lines in Mössbauer (Fortin), pure nuclear quadrupole resonance (NQR), or electron-spin resonance (ESR) spectra, or from X-ray or neutron diffraction studies;

5. The transformations to the cubic phase are accompanied by isotropic expansion of the lattices and large thermal parameters for the fourth-group atom;

6. The resulting cubic phases are often intensely colored and electrically conducting.

There seems at the present time no general theory available that would allow one to predict which compositions would exhibit these unusual behaviors (cf. ref. 33).

REFERENCES

1. Abrikosov, N. Kh., Novikova, S. I., Shelimova, L. E., and Zhdanova, V. V., *Izv. Akad. Nauk SSSR, Neorg. Mater.* **5**, 1895 (1969).
2. Abrikosov, N., Vasserman, A. N., and Poretskaya, I. V., *Dokl. Akad. Nauk SSSR* **123**, 279 (1958).
3. Agaev, K. A., and Semiletov, S. A., *Sov. Phys., Crystallogr. (Engl. Transl.)* **10**, 86 (1965).
4. Alexandrov, K. S., Besnosikov, B. V., and Posdnjakova, L. A., *Ferroelectrics* **12**, 197 (1976); *Chem. Abstr.* **86**, 36578j (1977).
5. Andersson, S., and Astrom, A., *NBS Spec. Publ.* **364**, *Solid State Chem. Proc. 5th Mater. Res. Symp.* (July, 1974).
6. Andrews, R. H., Ph. D. Thesis, University of London, (1977), quoted in refs. 34, 38.
7. Anon., *Chem. Eng. News*, 6 Aug., 1984, p. 20.
8. Anon., *Chem. Unser. Zeit* **18**(5), 179 (1984).
9. Avilov, A. S., Imamov, R. M., and Navasardyan, S. N., *Sov. Phys., Crystallogr. (Engl. Transl.)* **24**, 504 (1979).
10. Bachmann, R., and Schulz, H., *Solid State Ionics* **9**, **10**, 521 (1983).
11. Barrett, J., Bird, S. R. A., Donaldson, J. D., and Silver, J., *J. Chem. Soc. A*, p. 3105 (1971).
12. Bartell, L. S., *J. Chem. Educ.* **45**, 754 (1968).
13. Becker, P., ed., "Electron and Magnetization Densities in Molecules and Crystals," Plenum, New York, 1980.
14. Bedlivy, D., and Mereiter, K., *Acta Crystallogr., Sect. B* **B36**, 782 (1980).
15. Bernheim, R. A., Kempf, R. J., Gramas, J. V., and Skell, P. S., *J. Chem. Phys.* **43**, 196 (1965).
16. Bierly, J. N., Muldower, L., and Beckman, O., *Acta Metall.* **11**, 447 (1963).
17. Bills, J. L., and Snow, R. L., *J. Am. Chem. Soc.* **97**, 6340 (1975).
18. Bills, J. L., and Steed, S. P., *Inorg. Chem.* **22**, 2401 (1983).
19. Brown, I. D., in "Structure and Bonding in Crystals," M. O'Keefe and A. Navrotsky, eds., p. 1. Academic Press, New York, 1981.
20. Bulanova, G. G., Podlesskaya, A. V., Soboleva, L. V., and Soklakov, A. I., *Inorg. Mater. (Engl. Transl.)* **8**, 1698 (1972).
21. Burdett, J. K., "Molecular Shapes." Wiley, New York, 1980.
22. Burger, H., and Eujen, R., *Top. Curr. Chem.* **50**, 1 (1974).
23. Bystrom, A., *Arkiv Kemi, Mineral., Geol.* **25A**, No. 13 (1947).
24. Cambi, L., Ferrari, A., Coriselli, C., Solenghi, P., and Colla, C., *Gazz. Chim. Ital.* **65**, 1162 (1935).
25. Cavalca, L., Nardelli, M., and Grazioli, D., *Gazz. Chim. Ital.* **86**, 1041 (1956).

26. Chabin, M., and Gilletta, F., *J. Appl. Crystallogr.* **13**, 533 (1980).
27. Chambers, J. W., Heeg, M.-J., Janiak, C., Rausch, M. D., Schumann, H., and Zuckerman, J. J., *Abstr. 189th Am. Chem. Soc. Meet. Miami Beach, FL, Apr. 1985*.
28. Christensen, A. N., and Rasmussen, S. E., *Acta Chem. Scand.* **19**, 421 (1965).
29. Collotti, G., Conti, L., and Zocchi, R., *Acta Crystallogr.* **12**, 416 (1959).
30. Contreras, J. G., Seguel, G. V., Ungerer, B., Maier, W. F., and Hollander, F. J., *J. Mol. Struct.* **102**, 295 (1983).
31. Coppens, P., and Hall, M. B., eds., "Electron Distributions and the Chemical Bond." Plenum, New York, 1982.
32. Couch, D. A., Wilkins, C. J., Rossman, G. R., and Gray, H. B., *J. Am. Chem. Soc.* **92**, 307 (1970).
33. Cullen, D. L., and Lingafelter, E. C., *Inorg. Chem.* **10**, 1264 (1971).
34. Cusack, P. A., Smith, P. J., Donaldson, J. D., and Grimes, S. M., *Int. Tin Res. Inst. Publ.* **588** (1981).
35. Depmeier, W., Moller, A., and Klaska, K.-H., *Acta Crystallogr., Sect. B* **B36**, 803 (1980).
36. Desai, C. C., and Rai, J. L., *J. Cryst. Growth* **50**, 562 (1980).
37. Dickens, M. H., Hayes, W., Hutchings, M. T., and Smith, C., *J. Phys. C* **15**, 4043 (1982).
38. Donaldson, J. D., and Grimes, S. M., *Rev. Silicon, Germanium, Tin, Lead Compd.* **8**, 1 (1984).
39. Donaldson, J. D., Laughlin, D. H., Ross, S. D., and Silver, J., *J. Chem. Soc., Dalton Trans.*, p. 1985 (1973).
40. Donaldson, J. D., and Silver, J., *J. Chem. Soc., Dalton Trans.*, p. 666 (1973).
41. Donaldson, J. D., Silver, J., Hadjiminolis, S., and Ross, S. D., *J. Chem. Soc., Dalton Trans.*, p. 1500 (1975).
42. Dory, T. S., and Zuckerman, J. J., *J. Organomet. Chem.* **264**, 295 (1984).
43. Dory, T. S., Zuckerman, J. J., and Barnes, C. L., *J. Organomet. Chem.* **281**, C1 (1985).
44. Drago, R. S., *J. Chem. Educ.* **50**, 244 (1973).
45. Dutta, S. N., and Jeffrey, G. A., *Inorg. Chem.* **4**, 1363 (1965).
46. Edwards, A. J., and Khallow, K. I., *J. Chem. Soc., Chem. Commun.*, p. 50 (1984).
47. Eissenthal, K. B., Moss, R. A., and Turro, N. J., *Science* **225**, 1439 (1984).
48. Elliot, H., Hathaway, B. J., and Slade, B. C., *Inorg. Chem.* **5**, 669 (1966).
49. Fregerslev, S., and Rasmussen, S. E., *Acta Chem. Scand.* **22**, 2541 (1968).
50. Fujii, Y., Hoshino, S., Yamada, Y., and Shirane, G., *Phys. Rev. B* **9**, 4549 (1974).
51. Galy, J., Meunier, G., Andersson, S., and Astom, A., *J. Solid State Chem.* **13**, 142 (1975).
52. Gillespie, R. J., *Can. J. Chem.* **38**, 818 (1960).
53. Gillespie, R. J., *J. Chem. Educ.* **47**, 18 (1970).
54. Gillespie, R. J., "Molecular Geometry." Van Nostrand-Rheinhold, New York, 1972.
55. Gillespie, R. J., and Nyholm, R. S., *Q. Rev. Chem. Soc.* **11**, 339 (1957).
56. Goddard, W. A. III, *Science* **227**, 917 (1985).
57. Goldak, J., Barrett, C. S., Innes, D., and Youdelis, W., *J. Chem. Phys.* **44**, 3323 (1966).
58. Goldberg, I., and Herbstein, F. H., *Acta Crystallogr., Sect. B* **B28**, 400 (1972).
59. Goldberg, I., and Herbstein, F. H., *Acta Crystallogr., Sect. B* **B28**, 410 (1972).
60. Goldberg, I., and Herbstein, F. H., *Acta Crystallogr., Sect. B* **B29**, 246 (1973).
61. Goldberg, I., and Herbstein, F. H., *Isr. J. Chem.* **7**, VIP (1969).
62. Goldberg, I., Herbstein, F. H., and Kaftory, M., *Progr. Coord. Chem.* p. 238 (1968).
63. Goldberg, I., Herbstein, F. H., Kaftory, M., and Kapon, M., *Acta Crystallogr., Sect. A* **A28**, S 85 (1972).
64. Goldberg, I., Herbstein, F. H., and Reisner, M., *Isr. J. Chem.* **5**, 24p (1967).

65. Goodenough, J. B., cited in ref. 5, p. 14.
66. Harada, J., Sakata, M., Hoshino, S., and Hirotsu, S., *J. Phys. Soc. Jpn.* **40**, 212 (1976).
67. Harrison, P. G., *Coord. Chem. Rev.* **20**, 1 (1976).
68. Harrison, P. G., and Healy, M. A., *J. Organomet. Chem.* **51**, 153 (1973).
69. Harrison, P. G., and Zuckerman, J. J., *J. Am. Chem. Soc.* **92**, 2577 (1970).
70. Harrowfield, B. V., Dempster, A. J., Freeman, T. E., and Pilbrow, J. R., *J. Phys. C: Solid State Phys.* **6**, 2058 (1973).
71. Harrowfield, B. V., and Pilbrow, J. R., *J. Phys. C* **6**, 755 (1973).
72. Hashimoto, K., *J. Phys. Soc. Jpn.* **12**, 1423 (1957).
73. Hashimoto, K., and Hirakawa, K., *J. Phys. Soc. Jpn.* **11**, 716 (1956).
74. Hastie, J. W., Hauge, R. H., and Margrave, J. L., *Annu. Rev. Phys. Chem.* **21**, 475 (1970).
- 74a. Hathaway, B. J., *Struct. Bonding (Berlin)* **57**, 55 (1984).
75. Hathaway, B. J., and Slade, R. C., *J. Chem. Soc. A*, p. 85 (1968).
76. Haupt, H. J., Huber, F., and Preut, J., *Z. Anorg. Allg. Chem.* **408**, 209 (1974).
77. Heeg, M. J., Janiak, C., and Zuckerman, J. J., *J. Am. Chem. Soc.* **106**, 4295 (1984).
78. Herstein, F. H., *Z. Kristallogr* **157**, 39 (1981).
79. Herstein, F. H., and Kaftory, M., *Acta Crystallogr., Sect. B* **B28**, 405 (1972).
80. Hidaka, M., Okamoto, Y., and Zikumar, Y., *Phys. Status Solidi A* **79**, 263 (1983).
81. Hoppe, R., and Nowitzki, B., *Z. Anorg. Allg. Chem.* **509**, 145 (1984).
82. Howie, R. A., Moser, W., and Trevena, I. C., *Acta Crystallogr., Sect. B* **B28**, 2965 (1972).
83. Hutton, J., Nelmes, R. J., Meyer, G. M., and Eiriksson, V. R., *J. Phys. C* **12**, 5393 (1979).
84. Ioffe, A. I., and Nefefov, O. M., *Mendeleev Chem. J. (Engl. Transl.)* **24**, 58 (1979).
85. Isaacs, N. W., and Kennard, C. H. L., *J. Chem. Soc. A*, p. 386 (1969).
86. Ito, Y., and Koto, K., *Solid State Ionics* **9**, **10**, 527 (1983).
87. Ivanov-Emin, B. N., *Zh. Obshch. Khim.* **10**, 1813 (1940).
88. Janiak, C., Schumann, H., and Zuckerman, J. J., unpublished results.
89. Jones, P. G., *Chem. Soc. Rev.* **113**, 157 (1984).
90. Jørgensen, C. K., *Top. Curr. Chem.* **124**, 1 (1984).
91. Jutzi, P., Kohl, F., Hofmann, P., Krüger, C., and Tsay, Y.-H., *Chem. Ber.* **113**, 757 (1980).
92. Jutzi, P., Kohl, F., and Krüger, C., *Angew. Chem., Int. Ed. Engl.* **18**, 59 (1979).
93. Jutzi, P., Kohl, F., Krüger, C., Wolmershauser, G., Hofmann, P., and Stauffert, P., *Angew. Chem., Int. Ed. Engl.* **21**, 70 (1982).
94. Kafalas, J. A., and Mariano, A. N., *Science* **143**, 952 (1965).
95. Kannewurf, C. R., Kelly, A., and Cashman, R. J., *Acta Crystallogr.* **13**, 449 (1960).
96. Kimura, T., *Sci. Pap. Inst. Phys. Chem. Res. Jpn.* **73**, 31 (1979).
97. Kimura, T., and Sakurai, T., *J. Solid State Chem.* **34**, 369 (1980).
98. Klein, S., and Reinen, D., *J. Solid State Chem.* **32**, 311 (1980).
99. Kohl, F. X., Schluter, E., Jutzi, P., Krüger, C., Wolmershauser, G., Hoffman, P., and Stauffert, P., *Chem. Ber.* **117**, 1178 (1984).
100. Koshkin, V. M., Kukol', V. V., Mil'ner, A. P., Sabrodsii, Yu. R., and Katrunov, K. A., *Sov. Phys. Solid State (Engl. Transl.)* **19**, 939 (1977).
101. Koto, K., Schulz, H., and Huggins, R. A., *Solid State Ionics* **1**, 355 (1980).
102. Labbe, Ph., Frey, M., and Allais, G., *Acta Crystallogr., Sect. B* **B29**, 2204 (1973).
103. Lenhart, P. G., and Joesten, M. D., *Acta Crystallogr., Sect. B* **B36**, 1181 (1980).
104. Malen, E. N., in "Methods and Applications in Crystallographic Computing," (S. K. Hall and T. Ashida, eds.), p. 333. Oxford Univ. Press, London and New York, 1984.

105. Margrave, J. L., *Top. Curr. Chem.* **26**, 1 (1972).
106. Marstrander, A., and Møller, C. Kn., *Mat. Fys. Medd. K. Dan. Vidensk. Selsk.* **35**, No. 5 (1966).
107. Mauersberger, P., and Huber, F., *Acta Crystallogr., Sect. B*, **B36**, 683 (1980).
108. Mauersberger, P., and Huber, F., *Abstr. 3rd. Int. Conf. Organomet. Coord. Chem., Ge, Sn, Pb*, Univ. Dortmund (1980).
109. Mehl, M., and Nespal, W., *Z. Kristallogr. Kristallgeom. Kristallphys. Kristallchem.* **88**, 345 (1934).
110. Meizer, D., and Weiss, E., *J. Organomet. Chem.* **263**, 67 (1984).
111. Messer, D., *Z. Naturforsch., B Anorg. Chem. Org. Chem.* **33**, 366 (1978).
112. Mikolaichuk, A. G., Dutchak, Ya. I., and Freik, D. M., *Sov. Phys. Crystallogr. (Engl. Transl.)* **13**, 490 (1968).
113. Mikolaichuk, A. G., and Freik, D. M., *Sov. Phys. Crystallogr. (Engl. Transl.)* **11**, 2033 (1970).
114. Möller, A., and Felsche, J., *J. Appl. Crystallogr.* **15**, 247 (1982).
115. Möller, A., Wildermuth, G., and Felsche, J.,
116. Møller, C. Kn., *Mat.-Fys. Medd. K. Dan. Vidensk. Selsk.* **32**, No. 1 (1959).
117. Møller, C. Kn., *Mat.-Fys. Medd. K. Dan. Vidensk. Selsk.* **32**, No. 2 (1959).
118. Møller, C. Kn., *Mat.-Fys. Medd. K. Dan. Vidensk. Selsk.* **32**, No. 3 (1960).
119. Møller, C. Kn., *Nature (London)* **180**, 981 (1957).
120. Møller, C. Kn., *Nature (London)* **182**, 1436 (1957).
121. Moser, W., and Tevena, I. C., *J. Chem. Soc., Chem. Commun.*, p. 25 (1969).
122. Muetterties, E. L., and Wright, C. M., *Q. Rev. Chem. Soc.* **21**, 109 (1967).
123. Muldrew, L., *J. Nonmet.* **1**, 177 (1973).
124. Mullen, D., Heger, G., and Reinen, D., *Solid State Commun.* **17**, 1249 (1975).
- 124a. Muradyn, L. A., Sirota, M. L., Makarova, I. P., and Simonov, V. I., *Krystallografiya* **30**, 258 (1985).
125. Nefedov, O. M., Kolesnikov, S. P., Ioffe, A. I., *J. Organomet. Chem. Libr.* **5**, 181 (1977).
126. Nesterova, Y. M., Pashinkin, A. S., and Novoselova, A. V., *Russ. J. Inorg. Chem. (Engl. Transl.)* **6**, 1031 (1961).
127. Noda, Y., Ohba, S., Sato, S., and Saito, Y., *Acta Crystallogr., Sect. B* **B39**, 312 (1983).
128. Novikova, S. I., and Shelimova, L. E., *Sov. Phys., Solid State (Engl. Transl.)* **7**, 2052 (1966).
129. Ohta, H., Harada, J., and Hirotsu, S., *Solid State Commun.* **13**, 1969 (1973).
130. Okazaki, A., *J. Phys. Soc. Jpn.* **13**, 1151 (1958).
131. Orgel, L. E., *J. Chem. Soc.*, p. 3815 (1959).
132. Palatnik, L. S., and Levitin, V. V., *Dokl. Akad. Nauk SSSR* **96**, 975 (1954).
133. Panattoni, C., Bombieri, G., and Croatto, U., *Acta Crystallogr.* **21**, 823 (1966).
134. Petrov, I. I., and Imamov, R. M., *Sov. Phys., Crystallogr. (Engl. Transl.)* **15**, 134 (1970).
135. Platkhov, G. F., Pobedinskaya, E. A., Simonov, M. A., and Belov, N. V., *Sov. Phys., Crystallogr. (Engl. Transl.)* **15**, 928 (1971).
136. Poulsen, F. R., and Rasmussen, S. E., *Acta Chem. Scand.* **24**, 150 (1970).
137. Ramsdell, L. S., *Am. Mineral.* **10**, 281 (1925).
138. Raveau, B., *Rev. Silicon, Germanium, Tin, Lead, Compd.* **6**, 287 (1982).
139. Reinen, D., Freibell, C., and Reetz, K. P., *J. Solid State Chem.* **4**, 103 (1972).
140. Ruddick, J. N. R., *Rev. Silicon, Germanium, Tin, Lead, Compd.* **2**, 115 (1976).
141. Rundle, R. E., and Olson, D. H., *Inorg. Chem.* **3**, 596 (1964).
142. Saito, S., Endo, Y., and Hirota, E., *J. Chem. Phys.* **80**, 1327 (1984).
143. Sakata, M., Nishiwaki, T., and Harada, J., *J. Phys. Soc. Jpn.*, 232 (1979).
144. Sakurai, T., and Kobayashi, K., *Rikagaku Kenkyusho Hokoku* **55**, 69 (1979).
145. Sauka, Ya., *Zh. Fiz. Khim.* **25**, 41 (1951).

146. Scaife, D. E., Weller, P. F., and Fisher, W. G., *J. Solid State Chem.* **9**, 308 (1974).
147. Schmiedekamp, A., Cruickshank, D. W. J., Skaarup, S., Pulay, P., Hargittai, I., and Boggs, J. E., *J. Am. Chem. Soc.* **101**, 2002 (1979).
148. Schmitz-Dumont, O., and Bergerhoff, G., *Z. Anorg. Allg. Chem.* **283**, 314 (1956).
149. Schubert, K., and Fricke, H., *Z. Metallkd.* **44**, 457 (1953).
150. Schubert, K., and Fricke, H., *Z. Naturforsch.*, **A 6**, 781 (1951).
151. Schumann, H., *Zentralbl. Mineral. Geol. Palaeontol.* **33**, 122 (1933); *Chem. Abstr.*, **27**, 3127 (1933).
- 151a. Schumann, H., Janiak, C., Hahn, E., Loebel, J., and Zuckerman, J. J., *Angew. Chem.*, in press.
- 151b. Schumann, H., Janiak, C., Hahn, E., Loebel, J., Kolax, C., Heag, M.-J., Pickardt, J., Rauseh, M. D., and Zuckerman, J. J., unpublished results.
152. Shaplygin, I. S., and Lazarev, V. B., *Russ. J. Inorg. Chem. (Engl. Transl.)* **23**, 403 (1978).
153. Shiryayev, V. I., and Mironov, Y. F., *Russ. Chem. Rev. (Engl. Transl.)* **52**, 184, (1983).
154. Shustorovich, E., and Dobosh, P. A., *J. Am. Chem. Soc.* **101**, 4090 (1979).
155. Sidgwick, N. V., and Powell, H. M., *Proc. R. Soc., London Ser. A* **176**, 153 (1940).
156. Sillen, L. G., and Nylander, A.-L., *Ark. Kemi., Mineral. Geol.* **17A**, No. 4 (1943).
157. Smith, P. J., *J. Organomet. Chem. Libr.* **12**, 97 (1981).
- 157a. Smorodina, T. A., and Tsuranov, A. P., *Izv. Akad. Nauk SSSR, Neorg. Mater.* **20**, 1358 (1984).
158. Takagi, S., Joesten, M. D., and Lenhert, P. G., *Acta Crystallogr., Sect. B* **B31**, 1968 (1975).
159. Takagi, S., Joesten, M. D., and Lenhert, P. G., *Acta Crystallogr., Sect. B* **B32**, 326 (1976).
160. Takagi, S., Joesten, M. D., and Lenhert, P. G., *Acta Crystallogr., Sect. B* **B32**, 668 (1976).
161. Takagi, S., Joesten, M. D., and Lenhert, P. G., *Acta Crystallogr., Sect. B* **B32**, 1278 (1976).
162. Takagi, S., Joesten, M. D., and Lenhert, P. G., *J. Am. Chem. Soc.* **97**, 444 (1975).
163. Terpstra, P., and Westenbrink, H. K., *Verls. K. Ned. Akad. Wet. Amsterdam* **35**, 75 (1926); *Chem. Abstr.* **20**, 1735 (1926).
164. Troup, J. M., Estine, M. W., and Ziolo, R. F., in ref. 31, p. 285.
165. Urch, D. S., *J. Chem. Soc.*, p. 5775 (1964).
166. van Arkel, A. E., *Rec. Trav. Chim. Pays-Bas* **45**, 437 (1926).
167. van Driel, M., and Verweel, H. J., *Z. Kristallogr.* **95**, 308 (1936).
168. von Schnering, H. G., and Weidemeier, H., *Z. Kristallogr.* **156**, 143 (1981).
169. Weber, D., *Z. Naturforsch.*, **B 33**, 862 (1978).
170. Weidemeier, H., and von Schnering, H. G., *Z. Kristallogr.*, **148**, 295 (1978).
171. Wynne, K. J., *J. Chem. Educ.* **50**, 328 (1973).
172. Yamzin, I. I., Nozik, Yu. Z., and Belov, N. V., *Sov. Phys. Dokl. (Engl. Transl.)* **6**, 370 (1961).
173. Zachariasen, W. H., *Phys. Rev.* **40**, 917 (1932).
174. Zhukova, T. B., and Zaslavskii, A. I., *Sov. Phys. Crystallogr., (Engl. Transl.)* **12**, 28 (1967).
175. Ziolo, R. F., and Troup, J. M., *J. Am. Chem. Soc.* **105**, 229 (1983).
176. Zubieta, J. A., and Zuckerman, J. J., *Prog. Inorg. Chem.* **24**, 251 (1978).
177. Zuckerman, J. J., *Adv. Organomet. Chem.* **9**, 21 (1970).
178. Zuckerman, J. J., in "Chemical Mössbauer Spectroscopy" (R. H. Herber, ed.), p. 267. Plenum, New York, 1984.